# Probing the $R_{K^{(*)}}$ anomaly at a muon collider

Guo-yuan Huang,[1,*] Sudip Jana,[1,†] Farinaldo S. Queiroz,[2,3,‡] and Werner Rodejohann[1,§]

[1]*Max-Planck-Institut für Kernphysik, Saupfercheckweg 1, 69117 Heidelberg, Germany*
[2]*International Institute of Physics, Universidade Federal do Rio Grande do Norte, Campus Universitario, Lagoa Nova, Natal-RN 59078-970, Brazil*
[3]*Departamento de Fisica, Universidade Federal do Rio Grande do Norte, 59078-970 Natal, RN, Brasil and Millennium Institute for Subatomic Physics at the High Energy Frontier (SAPHIR), Santiago, Fernandez Concha 700, Chile*

(Received 8 March 2021; revised 26 March 2021; accepted 9 November 2021; published 11 January 2022)

The LHCb measurements of the $\mu/e$ ratio in $B \to K\ell\ell$ decays $(R_K)$ indicate a deficit with respect to the Standard Model prediction, supporting earlier hints of lepton universality violation observed in the $R_{K^{(*)}}$ ratio. Possible explanations of these $B$-physics anomalies include heavy $Z'$ bosons or scalar and vector leptoquarks mediating $b \to s\mu^+\mu^-$. We note that a muon collider can directly measure this process via $\mu^+\mu^- \to b\bar{s}$ and can shed light on the lepton nonuniversality scenario. Investigating currently discussed center-of-mass energies $\sqrt{s} = 3$, 6 and 10 TeV, we show that the parameter space of $Z'$ and leptoquark solutions to the $R_{K^{(*)}}$ anomalies can be mostly covered. Effective operators explaining the anomalies can be probed with the muon collider setup $\sqrt{s} = 6$ TeV and integrated luminosity $L = 4$ ab$^{-1}$.

DOI: 10.1103/PhysRevD.105.015013

## I. INTRODUCTION

Rare decays of mesons are sensitive to effects of heavy particles. Precision studies of many such decays have confirmed the CKM matrix as the source of flavor transitions in the Standard Model (SM) [1]. Nevertheless, longstanding hints for physics beyond the CKM paradigm exist. In particular, decay rates of charged and neutral $B$ mesons into kaons plus first and second generation charged leptons are notoriously away from precisely known SM calculations by $3.1\sigma$ [2–4]. A straightforward solution to these so-called $R_{K^{(*)}}$ puzzles is that there is new physics in the transition $b \to s\mu^+\mu^-$, which can be rewritten as $\mu^+\mu^- \to b\bar{s}$. For energy scales of $B$ decays this physics can be described by effective operators, which may stem from heavy particles mediating the transition. Essentially, there are only two possibilities at tree level. New $Z'$ bosons that couple to $b\bar{s}$ and $\mu^+\mu^-$ or hypothetical leptoquarks that couple to $\mu^- b$ and $\mu^+\bar{s}$.

This paper is about realizing the process $\mu^+\mu^- \to b\bar{s}(\bar{b}s)$ at high energy muon colliders. Those are currently under active discussion [5–21] as a possible future collider. While being interesting for Higgs physics, they would in particular be a powerful probe for anything new that likes muons. In particular, the option to test physics solutions for the anomalous magnetic moment of the muon, another longstanding problem involving muons [22–24], has been investigated. It has been shown that any new physics that may be responsible for explaining the $(g-2)_\mu$ results can be tested at future muon colliders [17–21]. Here we discuss the $B$ physics anomalies in the $R_K$ and $R_{K^*}$ ratios in terms of a $Z'$ and scalar as well as vector leptoquarks. The former mediates the process $\mu^+\mu^- \to b\bar{s}$ in an $s$-channel diagram, the latter in a $t$-channel diagram. Using the currently discussed setups of 3, 6, and 10 TeV center-of-mass energies [5,6], we show that both scenarios can be mostly covered. Our analysis takes THE dijet background from SM processes into account, and is independent of whether flavor tagging is included or not. Before turning to the analysis at the muon collider, we will shortly summarize the current situation of the anomalies and their main solutions.

## II. THEORETICAL INTERPRETATIONS OF THE $R_{K^{(*)}}$ ANOMALY

The ratios $R_K$ and $R_{K^*}$, relevant for testing the universality of the gauge-interactions in the lepton-sector, are defined as

*guoyuan.huang@mpi-hd.mpg.de
†sudip.jana@mpi-hd.mpg.de
‡farinaldo.queiroz@iip.ufrn.br
§werner.rodejohann@mpi-hd.mpg.de

$$R_K = \frac{\mathrm{BR}(B^+ \to K^+\mu^+\mu^-)}{\mathrm{BR}(B^+ \to K^+e^+e^-)}, \tag{1}$$

$$R_{K^\star} = \frac{\mathrm{BR}(B^0 \to K^{\star 0}\mu^+\mu^-)}{\mathrm{BR}(B^0 \to K^{\star 0}e^+e^-)}. \tag{2}$$

Due to highly suppressed hadronic uncertainties, such ratios are supposed to be theoretically clean and could thus be a "clean"-signal of BSM-physics. Very recently, the LHCb collaboration reported the results of $R_K$-measurement (in the region $q^2 \in [1.1, 6]$ GeV$^2$) as [2]

$$R_K^{\mathrm{LHCb}} = 0.846^{+0.042+0.013}_{-0.039-0.012}, \tag{3}$$

which indicates a $3.1\sigma$ discrepancy from its SM prediction [25,26]

$$R_K^{\mathrm{SM}} = 1.0003 \pm 0.0001. \tag{4}$$

Similarly, the LHCb Collaboration has also reported the results of $R_{K^*}$-measurement in two low-$q^2$ bins [3] ($q^2 \in [0.045, 1.1]$ GeV$^2$ and $q^2 \in [1.1, 6]$ GeV$^2$):

$$R_{K^*}^{\mathrm{LHCb}} = \begin{cases} 0.660^{+0.110}_{-0.070} \pm 0.024, \\ 0.685^{+0.113}_{-0.069} \pm 0.047, \end{cases} \tag{5}$$

which shows $2.2\sigma$ and $2.4\sigma$ deviations, respectively from their corresponding SM-predictions in each $q^2$ bin [27,28]:

$$R_{K^\star}^{\mathrm{SM}} = \begin{cases} 0.92 \pm 0.02, \\ 1.00 \pm 0.01. \end{cases} \tag{6}$$

Furthermore, Belle has also presented their results on $R_K$ [29] and $R_{K^*}$ [30]. However, there are comparatively larger uncertainties than for the LHCb measurements. There are in fact only a few BSM possibilities which could resolve these $R_{K^{(*)}}$-anomalies. Before entering details, it is quite important to mention that an explanation of $R_{K^{(*)}}$ by modifying the $b \to s\mu^+\mu^-$ decay anticipates a better global-fit to other observables, as compared to altering the $b \to se^+e^-$ decay [31].

The effective Lagrangian responsible for semileptonic $b \to s\mu^+\mu^-$-transitions can be expressed as ($V$ denotes the CKM-matrix)

$$\mathcal{L}^{\mathrm{NP}}_{b\to s\mu\mu} \supset \frac{4G_{\mathrm{F}}}{\sqrt{2}} V_{tb}V^*_{ts}(C^\mu_9 O^\mu_9 + C^\mu_{10}O^\mu_{10}) + \mathrm{H.c.} \tag{7}$$

with the relevant operators

$$O^\mu_9 = \frac{\alpha}{4\pi}(\bar{s}_{\mathrm{L}}\gamma_\mu b_{\mathrm{L}})(\bar{\mu}\gamma^\mu\mu),$$
$$O^\mu_{10} = \frac{\alpha}{4\pi}(\bar{s}_{\mathrm{L}}\gamma_\mu b_{\mathrm{L}})(\bar{\mu}\gamma^\mu\gamma_5\mu). \tag{8}$$

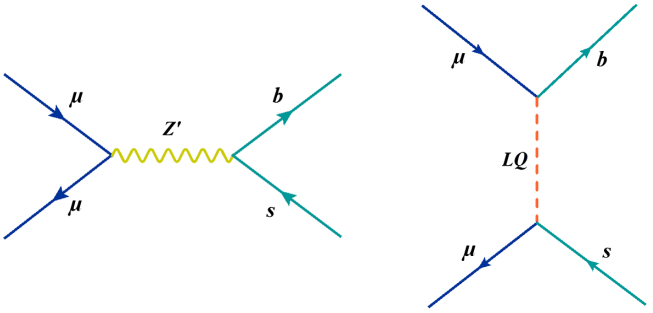


FIG. 1. Tree-level processes at a muon collider directly related to $R_{K^{(*)}}$: $Z'$ or leptoquark.

Using these operators to explain the anomalies leads to best-fit values of the Wilson-coefficients $C_9 = -C_{10} = -0.43$, with the $1\sigma$ range being $[-0.50, -0.36]$ [31,32].

## III. MODELS WITH $Z'$

Let us now discuss an explicit new-physics realization for explaining the $B$-anomalies in neutral-currents. As a prototypical-model (a partial list of references is [33–55]), we consider a $Z'$ which dominantly couples to $bs$ and $\mu^+\mu^-$, via left-handed currents.[1] One can achieve this by extending the SM with an extra $U(1)$ gauge group, which brings in a new $Z'$ boson having a nonuniversal lepton-coupling and a flavor-changing quark-coupling. Here, we concentrate solely on the Lagrangian-part relevant for $b \to s\mu^+\mu^-$-transitions, namely

$$\mathcal{L}_{Z'} \supset (\lambda^{\mathrm{Q}}_{ij}\bar{d}^i_{\mathrm{L}}\gamma^\mu d^j_{\mathrm{L}} + \lambda^{\mathrm{L}}_{\alpha\beta}\bar{\ell}^\alpha_{\mathrm{L}}\gamma^\mu \ell^\beta_{\mathrm{L}})Z'_\mu, \tag{9}$$

where $\ell^i$ and $d^i$ denote the different generations of charged-lepton and down-type quark states, respectively.

Integrating out the $Z'$ field, one can obtain the effective-Lagrangian as:

$$\begin{aligned}\mathcal{L}^{\mathrm{eff}}_{Z'} &= -\frac{1}{2M^2_{Z'}}(\lambda^{\mathrm{Q}}_{ij}\bar{d}^i_{\mathrm{L}}\gamma_\mu d^j_{\mathrm{L}} + \lambda^{\mathrm{L}}_{\alpha\beta}\bar{\ell}^\alpha_{\mathrm{L}}\gamma_\mu \ell^\beta_{\mathrm{L}})^2 \\ &\supset -\frac{1}{2M^2_{Z'}}[(\lambda^{\mathrm{Q}}_{23})^2(\bar{s}_{\mathrm{L}}\gamma_\mu b_{\mathrm{L}})^2 \\ &\quad + 2\lambda^{\mathrm{Q}}_{23}\lambda^{\mathrm{L}}_{22}(\bar{s}_{\mathrm{L}}\gamma_\mu b_{\mathrm{L}})(\bar{\mu}_{\mathrm{L}}\gamma^\mu\mu_{\mathrm{L}}) + \mathrm{H.c.}].\end{aligned} \tag{10}$$

Now one can find the relevant Wilson-coefficients at tree-level [cf. left-panel of Fig. 1] by matching onto the effective-Lagrangians for the low-energy observables at the scale ($\mu = M_{Z'}$) as

[1]Right-handed currents in the lepton-sector actually worsen the compatibility of $R_{K^{(*)}}$ explanation with the $\Delta M_s$ (mass-differences of neutral $B$-mesons) measurement [56], since they demand a larger Wilson-coefficient.

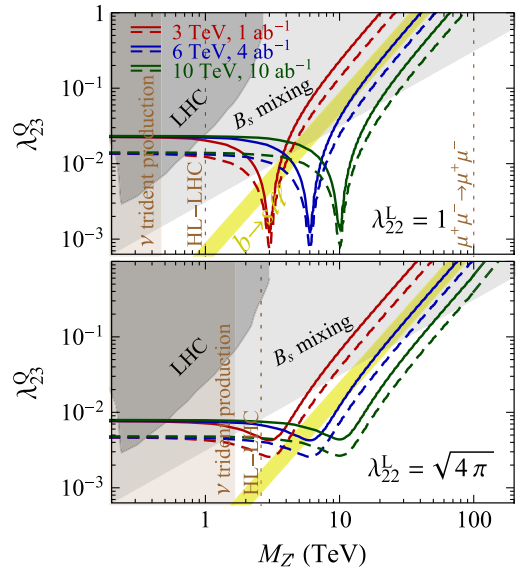


FIG. 2. The sensitivity contours for the $Z'$ model with $\lambda^{\rm L}_{22}=1$ (upper panel) and $\lambda^{\rm L}_{22}=\sqrt{4\pi}$ (lower panel) via the process $\mu^+\mu^-\to b\bar{s}$ at muon colliders with the following setups: $\sqrt{s}=3$ TeV and $L=1$ ab$^{-1}$ (red curves), $\sqrt{s}=6$ TeV and $L=4$ ab$^{-1}$ (blue curves), as well as $\sqrt{s}=10$ TeV and $L=10$ ab$^{-1}$ (green curves). The $2\sigma$ parameter space favored by a fit of $B$ anomalies is shown as the yellow band [32]. Dashed (solid) curves stand for the case with (without) flavor tagging. The $B_s$ mixing bounds are given as gray shaded regions [56]. The limits from neutrino trident production are recast as brown shaded regions [63]. The regions disfavored by LHC dimuon resonance searches are shown as black shaded regions, rescaled from Ref. [64]. This limit is overestimated as all light quarks are assumed to couple identically to $Z'$. The projected sensitivity of HL-LHC is given by the vertical dotted lines near 1 TeV [65]. The $\mu^+\mu^-\to\mu^+\mu^-$ process at the muon collider can probe all $M_{Z'}$ values smaller than 100 TeV with order one $\lambda^{\rm L}_{22}$ [20]. These are shown as two vertical lines near 100 TeV.

$$C^{\mu}_9=-C^{\mu}_{10}=-\frac{\pi}{\sqrt{2}G_{\rm F}M^2_{Z'}\alpha}\left(\frac{\lambda^{\rm Q}_{23}\lambda^{\rm L}_{22}}{V_{tb}V^*_{ts}}\right). \tag{11}$$

However, as shown, e.g., in Refs. [56,57], this $Z'$-explanation of $R_{K^{(*)}}$ anomaly is under tight constraints from several theoretical and experimental limits allowing a narrow mass-range for $Z'$ boson [cf. the yellow band in Fig. 2]. There are several dedicated $Z'$-searches at the LHC looking at dimuon or dijet [58,59] signatures. The reliance on parton distribution functions of bottom-quarks for production in our scenario dilutes the impact of current LHC-searches. On the other hand, a very stringent bound on our $Z'$ originates from its flavor-changing coupling, which generates an additional contribution to $B_s-\bar{B}_s$ mixing [56,57]. Note that other constraints, such as BR$(B\to K\bar{\nu}\nu)$ [60] or muon $g-2$ [61,62], are much weaker. In addition, there will be constraints from the measurement of neutrino-trident production [63]. All these constraints are summarized in Fig. 2.

## IV. MODELS WITH LEPTOQUARKS

In order to address the $R_{K^{(*)}}$-anomaly, there is another popular class of models (a partial list of references is [66–88]) in which leptoquarks are applied. Here we briefly review these simplified models that can accommodate the $R_{K^{(*)}}$-anomaly. There are only four scalar leptoquarks which can interact with the SM-fermions at renormalizable level. Interestingly, $S_3\sim(3,3,-1/3)$ can simultaneously address $R_K$ and $R_{K^*}$ and whose constraints are not in conflict with the experimental data [89,90]. Similarly, the vector leptoquark $U_1\sim(3,1,2/3)$ can also provide a good fit for the $R_{K^{(*)}}$-anomaly. Note that it requires a proper UV-completion for theoretical consistency. Here we focus mainly on the scalar case, delegating details of the vector leptoquark case to the Appendix B.

The relevant Lagrangian for $S_3$ can be written as:

$$\mathcal{L}_{S_3}=-M^2_{S_3}|S^a_3|^2+y^{\rm LQ}_{i\alpha}\overline{Q^{ci}}(\epsilon\sigma^a)L^{\alpha}S^a_3+{\rm H.c.}, \tag{12}$$

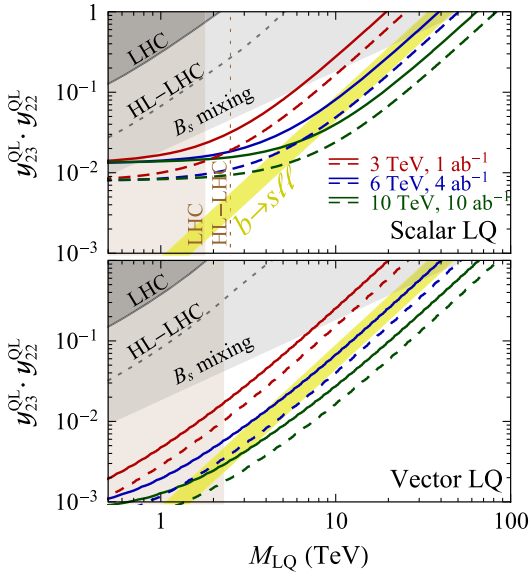


FIG. 3. The sensitivity contours for $S_3$ (upper panel) and $U_1$ (lower panel) leptoquark models via the process $\mu^+\mu^-\to b\bar{s}$ at muon colliders with the following setups: $\sqrt{s}=3$ TeV and $L=1$ ab$^{-1}$ (red curves), $\sqrt{s}=6$ TeV and $L=4$ ab$^{-1}$ (blue curves), as well as $\sqrt{s}=10$ TeV and $L=10$ ab$^{-1}$ (green curves). The $2\sigma$ parameter space favored by a fit of $B$ anomalies is shown as the yellow band [32]. Dashed (or solid) curves stand for the case with (or without) the flavor tagging. The $B_s$ mixing bound on leptoquark is given as gray shaded regions [57]. The constraints by LHC searches of leptoquark pair production (or indirect high-energy tails $q\bar{q}\to\mu^+\mu^-$) as well as the future projection of high-luminosity LHC [94,96] are given by the brown (or black) shaded region and the dotted line, respectively. Note that for $U_1$ leptoquark, the assumption $\mathcal{L}\supset\kappa g_s U^{\dagger\mu}_1 G_{\mu\nu}U^{\nu}_1$ with $\kappa=1$ has been made in deriving the constraints from leptoquark pair production [96].

with lepton and quark-doublets $L^\alpha = (\nu_L^\alpha, \ell_L^\alpha)^T$ and $Q^i = (V_{ji}^* u_L^j, d_L^i)^T$, and Pauli-matrices $\sigma^a$ ($a = 1, 2, 3$; $\epsilon = i\sigma^2$). The leptoquark contributes to the Wilson-coefficients at tree-level [cf. Fig. 1] and one can identify:

$$C_9^\mu = -C_{10}^\mu = \frac{\pi}{\sqrt{2} G_F M_{S_3}^2 \alpha} \left( \frac{y_{32}^{LQ} y_{22}^{LQ*}}{V_{tb} V_{ts}^*} \right). \quad (13)$$

This explanation of the $R_{K^{(*)}}$ anomaly also faces several theoretical and experimental constraints. The same combination of Yukawa-couplings leads to $B_s - \bar{B}_s$ mixing at one-loop level [57,91,92]. This sets an upper bound on the Yukawa-couplings as a function of the leptoquark mass as shown in Fig. 3. Due to the loop-nature of this constraint, it is much weaker compared to the $Z'$ scenario. There are several relevant direct LHC searches. Pair-production via gluon-gluon fusion processes dominates and the subsequent decay into $\mu j$ can be looked for. A stringent limit from a dedicated LHC search using $\mu\mu jj$ signals exists [93]. Recently, Ref. [94] has worked out in detail the prospect of probing the $S_3$ leptoquark at current and future runs of the LHC. Based on that analysis masses up to 1.8 TeV are excluded at 95% confidence level from 13 TeV LHC data with an integrated luminosity of $\mathcal{L} = 140$ fb$^{-1}$, whereas HL-LHC (with 3 ab$^{-1}$ integrated luminosity) can probe up to 2.5 TeV. The minimal constraints without assuming additional flavor structures from indirect high-$p_T$ searches of $q\bar{q} \to \mu^+\mu^-$ are less competitive [95–97]. All these constraints are summarized in Fig. 3.

## V. IMPLICATIONS OF $R_{K^{(*)}}$ ANOMALY AT A MUON COLLIDER

The transition of $b \to s\mu^+\mu^-$ in meson decays is directly applicable in a muon collider via $\mu^+\mu^- \to b\bar{s}$. This simple two-body scattering allows to directly test any explanation for the anomalous $R_{K^{(*)}}$ ratios, and we utilize it to study the sensitivity on the representative explanations of the anomalies, i.e., a $Z'$ and scalar as well as vector leptoquarks.

The Feynman diagrams of the relevant processes are depicted in Fig. 1. For the $Z'$ model, we have an $s$-channel process, and a resonance enhancement is available when the center-of-mass energy $\sqrt{s}$ is near the $Z'$ mass $M_{Z'}$. In contrast, the $S_3$ leptoquark mediates a $t$-channel process.

Besides the explicit realization of the cross section, we can describe the situation in an effective language. When the $Z'$ or leptoquark mass is larger than the center-of-mass energy, the operators with coefficients $C_9^\mu$ and $C_{10}^\mu$ are responsible for the transition. The cross section of $\mu^+\mu^- \to b\bar{s}$ is then

$$\sigma(s) = \frac{G_F^2 \alpha^2 |V_{tb} V_{ts}^*|^2 s}{8\pi^3} (|C_9^\mu|^2 + |C_{10}^\mu|^2). \quad (14)$$

Taking the best-fit scenario of $B$ anomalies, $C_9^\mu = -C_{10}^\mu = -0.43$, we obtain the event number of $bs$ final states $\sigma(s) \cdot L$ ($L$ being the luminosity) as

$$\#\text{signal} \simeq 10^3 \left( \frac{\sqrt{s}}{6\ \text{TeV}} \right)^2 \left( \frac{L}{4\ \text{ab}^{-1}} \right).$$

As a naive comparison, we obtain the relevant SM background in the form of quark dijets (ignoring flavor tagging, see below), which turns out to be $1.2 \times 10^5 \cdot (6\ \text{TeV}/\sqrt{s})^2 \cdot (L/4\ \text{ab}^{-1})$. The signal exceeds the fluctuation of SM background at around $3\sigma$ level, which is very encouraging. The signal-to-background ratio is roughly proportional to $s^2$; therefore to enhance the sensitivity to the effective operators, larger $\sqrt{s}$ is preferred. With $\sqrt{s} = 10$ TeV and $L = 10$ ab$^{-1}$, values of $|C_9^\mu| = |C_{10}^\mu|$ as small as 0.16 can be reached at $3\sigma$ level, which covers the $2\sigma$ range of $|C_9^\mu| = |C_{10}^\mu| \in [0.29, 0.57]$ even without the flavor tagging. For comparison, the current LHC (projected HL-LHC) limit on the coefficients of effective operators reads $|C_9^\mu| = |C_{10}^\mu| < 100(39)$ [95]. These hadron collider bound on the effective operators is set by searching for the high-$p_T$ tails of the dimuon spectrum, which is not as efficient as a muon collider. In the Appendix C we discuss more details on the muon-collider sensitivity on effective operators. Before discussing the explicit realizations of the process, we consider general background issues.

The dijet signal of the $bs$ final state is contaminated by $\mu^+\mu^- \to jj$, where $j$ can be $u$, $d$, $s$, $c$ and $b$, due to imperfect flavor reconstruction. The sensitivity depends on the $b$-jet tagging efficiency as well as the mistag rate (identifying a light quark jet as a $b$-jet). In this work, we assume an experimental configuration with a $b$-jet tagging efficiency $\epsilon_b = 70\%$ [8] and mistag rates $\epsilon_{uds} = 1\%$ for light quarks and $\epsilon_c = 10\%$ for $c$ quarks [98–100]. We require in our analysis that one jet is tagged as a $b$ jet, while the other is not. We continue with some comments on the backgrounds:

(i) $\mu^+\mu^- \to u\bar{u}, d\bar{d}, s\bar{s}, c\bar{c}$: With the tagging requirement, the total cross section for these processes will be reduced by a factor of $2\epsilon_{uds,c} \cdot (1 - \epsilon_{uds,c})$, where the factor 2 originates from two choices of tagging.

(ii) $\mu^+\mu^- \to b\bar{b}$: To pass our event criteria, one $b$-jet is required not to be $b$-tagged, and the cross section is reduced by a factor $2\epsilon_b \cdot (1 - \epsilon_b)$. Note that one could likely further optimize the selection criteria until a higher signal-to-noise ratio is obtained.

In addition, there could be background contributions from top quarks. However, their identification relies crucially on the tagging of a $b$ quark in their decay $t \to Wb$. Above TeV energies, the top-antitop final states are highly boosted, such that multiple final jets may overlap [101]. However, the fractional momentum carried by the $b$-tagged jet always lies below $\sqrt{s}/2$, which should be well separated from the prompt $b$ jet [99] with proper

energy cuts. Thus, in our analysis we assume the top background to be negligible. An inclusion should not affect our results much, because other dijet backgrounds remain dominant.

For illustration, we will investigate three collider setups with center-of-mass energies and luminosities, namely $(\sqrt{s}, L) = (3\ \text{TeV}, 1\ \text{ab}^{-1})$, $(6\ \text{TeV}, 4\ \text{ab}^{-1})$ and $(10\ \text{TeV}, 10\ \text{ab}^{-1})$. For completeness, results with and without flavor tagging will be given. We will use FeynCalc [102–104] and FeynArts [105] for the numerical calculations of the scattering amplitudes.

For simplicity, we perform the analysis at the parton level. An angular cut $10° < \theta < 170°$ on the final state jets will be implemented. Since there are no divergent $t$-channel contributions, a slightly stricter or looser angular cut will not affect the final sensitivity much. The signal jets are monoenergetic with $E_j = \sqrt{s}/2$. At the parton level, no additional cut on the energy needs to be considered. The statistical significance is measured by

$$\chi^2 = \sum_i \frac{(N_i - \tilde{N}_i)^2}{N_i + \epsilon^2 \cdot N_i^2}, \tag{15}$$

where $N_i$ is the expected total event number of signal and backgrounds, and $\tilde{N}_i$ is the assumed event number observed by the experiment. The sensitivity can be generated by setting $\tilde{N}_i$ to be SM backgrounds only, i.e., a null signal. Further, $\epsilon$ denotes the possible systematic uncertainty, which will be fixed as 0.1% [13] in our work. Setting $\epsilon$ to a higher value of 1%, which is comparable to the signal-to-background ratio without flavor tagging (see Appendix A for more details), will dilute the significance. Nevertheless, after the flavor tagging procedure, the effect of systematic uncertainty is not significant as long as $\epsilon$ stays below 2%. The index $i$ sums over polar angles, for which we take a bin size of $\cos\theta$ as 0.1. We highlight that we have checked that a finer binning does not improve the significance much, as the spectrum shape is already well contained with our choice.

The final sensitivity contours are shown in Fig. 2 (for $Z'$) and Fig. 3 (for leptoquark), where the red, blue and green curves correspond to the muon collider setups $(\sqrt{s}, L) = (3\ \text{TeV}, 1\ \text{ab}^{-1})$, $(6\ \text{TeV}, 4\ \text{ab}^{-1})$ and $(10\ \text{TeV}, 10\ \text{ab}^{-1})$, respectively. The solid (or dashed) curves stand for the case without (or with) flavor tagging. For comparison, the parameter regions explaining the $R_{K^{(*)}}$ anomaly for $Z'$ and leptoquark models are given as yellow bands. For the $Z'$ case, there is a resonance near the center-of-mass energy. The width of the resonance depends on the couplings $\lambda^{\text{L}}_{22}$ and $\lambda^{\text{Q}}_{23}$ via $\Gamma = (2|\lambda^{\text{L}}_{22}|^2 + 3|\lambda^{\text{Q}}_{23}|^2)/(12\pi)$. For small $\lambda^{\text{Q}}_{23}$, the width is dominated by our choice of $\lambda^{\text{L}}_{22}$. If the $Z'$ and leptoquark masses are much smaller than the center-of-mass-energy, the sensitivity curves do not depend on the mediator mass. In this case, since the collider setups have luminosities $L \propto \sqrt{s}^2$, the event number $\sigma(s) \cdot L$ will be a constant for $\sigma(s) \propto s^{-1}$ at large momentum transfer. At large $Z'$ and leptoquark masses, the mediator is decoupled, and the contours of the two models converge to each other. We note that in this regime the results will be applicable to any effective theory described by Eq. (7). Some further comments are in order:

(i) Due to the constraints from neutrino trident production and $B_s$ mixing, the parameter space is very limited for the $Z'$ scenario. The coverage of parameter space by the muon collider depends on the value of $\lambda^{\text{L}}_{22}$. It is worth noting that the dimuon signal from $\mu^+\mu^- \to \mu^+\mu^-$ is able to cover all the $\lambda^{\text{L}}_{22}$ and $M_{Z'}$ values explaining the $B$ anomalies [20]. In this case, the inclusion of $\mu^+\mu^- \to b\bar{s}$ helps to clarify that the new physics is indeed what causes the $B$ anomalies. The $B_s$ mixing data prefers larger $\lambda^{\text{L}}_{22}$ values. If we take $\lambda^{\text{L}}_{22} = 1$, a window between the projection for the HL-LHC and the muon collider setup with $\sqrt{s} = 3$ TeV may survive. But this window is expected to be covered by means of radiative return, i.e., $\mu^+\mu^- \to bs\gamma$. For the extreme case $\lambda^{\text{L}}_{22} = \sqrt{4\pi}$ where more parameter space is valid to explain the $R_{K^{(*)}}$ anomaly, the muon collider with $\sqrt{s} = 6$ TeV will rule out most of the favored parameter space. Combining the HL-LHC and the muon collider sensitivities we observe that there is still a corner of the parameter space left.

(ii) For the case of leptoquarks, most of the parameter space will be probed with the muon collider $\sqrt{s} = 6$ TeV and $L = 4\ \text{ab}^{-1}$. Only a tiny window around 3 TeV for scalar-leptoquarks may survive, which can be of course covered by a larger integrated luminosity (e.g., with $L = 16\ \text{ab}^{-1}$ for $\sqrt{s} = 6$ TeV no space will be left). The parameter space of vector leptoquark and coefficients of effective operators can be fully covered with $\sqrt{s} = 6$ TeV and $L = 4\ \text{ab}^{-1}$.

## VI. CONCLUSION

Processes with muons are a reliable source of anomalies which could lead to the discovery of long-awaited new physics beyond the Standard Model. A muon collider is then an ideal machine to probe these effects further. Here we have focused on the highly interesting $R_K$ and $R_{K^*}$ ratios, which are object to intense studies in terms of heavy

$Z'$ bosons and leptoquarks. We have demonstrated that the parameter space of such models can be mostly covered at currently discussed muon collider setups, which adds exciting physics potential to these facilities.

## ACKNOWLEDGMENTS

G.-Y. H was supported by the Alexander von Humboldt Foundation. F. S. Q. is supported by the Sao Paulo Research Foundation (FAPESP) through Grant No. 2015/158971, ICTP-SAIFR FAPESP Grant No. 2016/01343-7, CNPq Grants No. 303817/2018-6 and No. 421952/2018-0, and the Serrapilheira Institute (Grant No. Serra-1912-31613).

## APPENDIX A: SIGNAL-TO-BACKGROUND RATIO

In Fig. 4, an illustration of the signal-to-background ratio before (solid) and after (dashed) flavor tagging is given for the leptoquark model with parameter sets explaining the $B$ anomalies $y_{23}^{\mathrm{LQ}} \cdot y_{22}^{\mathrm{LQ}} = 0.02$ and $M_{S_3} = 5$ TeV (red curves), as well as $y_{23}^{\mathrm{LQ}} \cdot y_{22}^{\mathrm{LQ}} = 0.7$ and $M_{S_3} = 30$ TeV (blue curves). One can observe that with our flavor tagging assumptions, the signal-to-background ratio can be enhanced by one order of magnitude. Considerable variations of the signal-to-background ratio over the polar angle can be noticed for the case with $M_{S_3} = 5$ TeV, which helps to preserve the statistical significance against a possibly large systematic uncertainty. However, for the case with $M_{S_3} = 30$ TeV, the leptoquark is basically decoupled, and the signal-to-background ratio is nearly a constant if we do not distinguish quark and antiquark. A possible tagging of the $b$ quark charge [106] will distort the flat signal-to-background ratio.

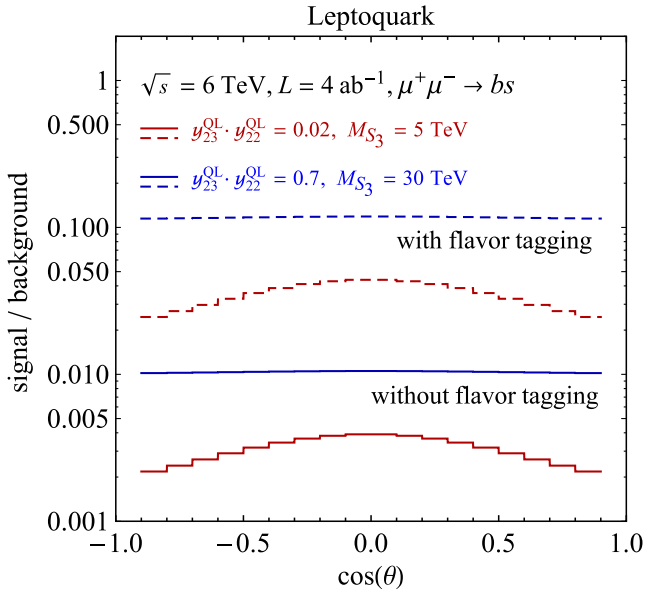


FIG. 4. The ratio of leptoquark signal to SM background at a muon collider with $\sqrt{s} = 6$ TeV and $L = 4$ ab$^{-1}$. The red curves stand for the scenario $y_{23}^{\mathrm{LQ}} \cdot y_{22}^{\mathrm{LQ}} = 0.02$ and $M_{S_3} = 5$ TeV, where the leptoquark mass is comparable to the collision energy. The blue curves stand for the scenario $y_{23}^{\mathrm{LQ}} \cdot y_{22}^{\mathrm{LQ}} = 0.7$ and $M_{S_3} = 30$ TeV. Here the leptoquark can safely be integrated out, and the scattering is described by effective operators. The case with (without) flavor tagging is shown as dashed (solid) curves.

## APPENDIX B: VECTOR LEPTOQUARK

The Lagrangian describing the $U_1$ vector-leptoquark reads

$$\mathcal{L}_{U_1} = -M_{U_1}^2 |U_1|^2 + y_{i\alpha}^{\mathrm{LQ}} \overline{Q^i} \gamma_\mu L^\alpha U_1^\mu + \mathrm{H.c.} \tag{B1}$$

The corresponding contribution to the Wilson-coefficients at tree-level is similar to the $S_3$ leptoquark, namely

$$C_9^\mu = -C_{10}^\mu = \frac{\pi}{\sqrt{2} G_{\mathrm{F}} M_{U_1}^2 \alpha} \left( \frac{y_{32}^{\mathrm{LQ}} y_{22}^{\mathrm{LQ}*}}{V_{tb} V_{ts}^*} \right). \tag{B2}$$

When the leptoquark mass is much larger than the colliding energy, the effects induced by $S_3$ and $U_1$ leptoquarks at muon colliders will be indistinguishable. When the leptoquark mass is negligible compared to the colliding energy, the $t$-channel exchange of $U_1$ leptoquark will enhance the cross section significantly by a factor of $1/(Q^2 + M_{U_1}^2)^2$. However, for the $S_3$ case, the scalar coupling, which reverses the chirality, does not feature a $t$-channel enhancement. This can be easily seen: the vertex for the scalar coupling contributes a factor $\mathrm{Tr}(\not{p}\not{k}) = 4p \cdot k \propto Q^2$ with $p$ and $k$ being the four momentum of initial and final fermions coupled to the leptoquark, and the $t$-channel enhancement when $Q^2 \to 0$ is therefore canceled. As a consequence, in Fig. 3 of the main manuscript, we have better sensitivities at small masses for the vector leptoquark.

## APPENDIX C: SENSITIVITY TO EFFECTIVE OPERATORS

In Fig. 5, we show the $3\sigma$ sensitivity of muon colliders to $|C_9^\mu|^2 + |C_{10}^\mu|^2$ as a function of the colliding energy $\sqrt{s}$. The yellow band corresponds to the $2\sigma$ range favored by the global analysis, namely $C_9^\mu = -C_{10}^\mu \in [0.29, 0.57]$. The blue region (dashed blue curve) shows the excluded values of $|C_9^\mu|^2 + |C_{10}^\mu|^2$ for a given colliding energy $\sqrt{s}$ assuming only the Standard Model background is observed without (with) flavor tagging. With the setup $\sqrt{s} = 6$ TeV and $L = 4$ ab$^{-1}$, the best-fit point $C_9^\mu = -C_{10}^\mu = -0.43$ can be reached without the flavor tagging. We note that with the colliding energy $\sqrt{s} \gtrsim 6$ TeV and the flavor tagging the entire $2\sigma$ range of parameter space favored by the $B$ anomalies can be covered.

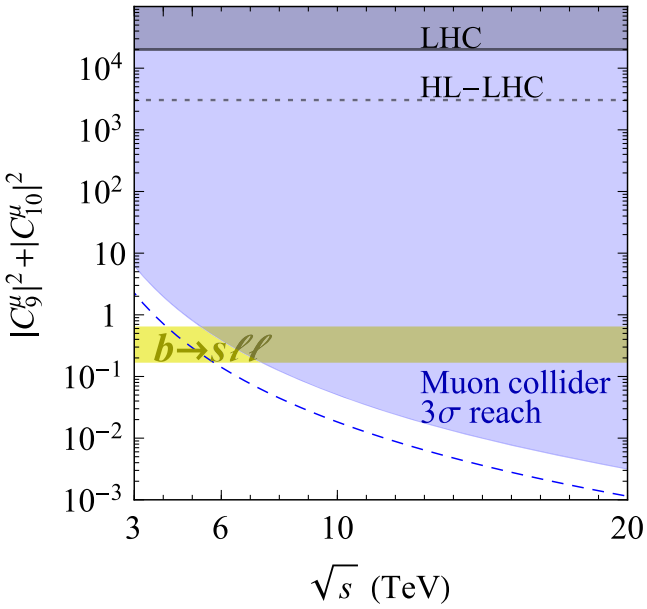


FIG. 5. The sensitivity of muon colliders to the square sum of effective operator coefficients $|C_9^\mu|^2 + |C_{10}^\mu|^2$ as a function of the colliding energy $\sqrt{s}$. The luminosity has been assumed to satisfy the benchmark value $L = 4\ \text{ab}^{-1} \cdot [\sqrt{s}/(6\ \text{TeV})]^2$. The blue region (the dashed blue curve) is the $3\sigma$ exclusion parameter space assuming no excess beyond the Standard Model background has been observed without (with) the flavor tagging, while the yellow band indicates the $2\sigma$ range favored by the global fit of $B$ anomalies assuming $C_9^\mu = -C_{10}^\mu$ [31,32]. The LHC limit and the HL-LHC projection by looking for high-energy dimuon tails, assuming only the $bs\mu\mu$ couplings, are given as black shaded region and dotted line, respectively [93].


[1] P. A. Zyla *et al.* (Particle Data Group Collaboration), Review of particle physics, Prog. Theor. Exp. Phys. **2020**, 083C01 (2020).

[2] R. Aaij *et al.* (LHCb Collaboration), Test of lepton universality in beauty-quark decays, arXiv:2103.11769.

[3] R. Aaij *et al.* (LHCb Collaboration), Test of lepton universality with $B^0 \to K^{*0}\ell^+\ell^-$ decays, J. High Energy Phys. 08 (2017) 055.

[4] R. Aaij *et al.* (LHCb Collaboration), Search for Lepton-Universality Violation in $B^+ \to K^+\ell^+\ell^-$ Decays, Phys. Rev. Lett. **122**, 191801 (2019).

[5] Muon Collider Collaboration Meeting, https://indico.cern.ch/event/930508/.

[6] Potential Goal for First Period, https://indico.cern.ch/event/930508/contributions/3920339/.

[7] K. Cheung and Z. S. Wang, Physics potential of a muon-proton collider, Phys. Rev. D **103**, 116009 (2021).

[8] W. Liu and K.-P. Xie, Probing electroweak phase transition with multi-TeV muon colliders and gravitational waves, J. High Energy Phys. 04 (2021) 015.

[9] T. Han, S. Li, S. Su, W. Su, and Y. Wu, Heavy Higgs bosons in 2HDM at a muon collider, Phys. Rev. D **104**, 055029 (2021).

[10] M. Chiesa, F. Maltoni, L. Mantani, B. Mele, F. Piccinini, and X. Zhao, Measuring the quartic Higgs self-coupling at a multi-TeV muon collider, J. High Energy Phys. 09 (2020) 098.

[11] A. Costantini, F. De Lillo, F. Maltoni, L. Mantani, O. Mattelaer, R. Ruiz, and X. Zhao, Vector boson fusion at multi-TeV muon colliders, J. High Energy Phys. 09 (2020) 080.

[12] T. Han, D. Liu, I. Low, and X. Wang, Electroweak couplings of the Higgs boson at a multi-TeV muon collider, Phys. Rev. D **103**, 013002 (2021).

[13] T. Han, Z. Liu, L.-T. Wang, and X. Wang, WIMPs at high energy muon colliders, Phys. Rev. D **103**, 075004 (2021).

[14] P. Bandyopadhyay and A. Costantini, The *Obscurum* Higgs at Colliders, Phys. Rev. D **103**, 015025 (2021).

[15] J. Gu, L.-T. Wang, and C. Zhang, An unambiguous test of positivity at lepton colliders, arXiv:2011.03055.

[16] R. Capdevilla, F. Meloni, R. Simoniello, and J. Zurita, Hunting wino and higgsino dark matter at the muon collider with disappearing tracks, J. High Energy Phys. 06 (2021) 133.

[17] R. Capdevilla, D. Curtin, Y. Kahn, and G. Krnjaic, A guaranteed discovery at future muon colliders, Phys. Rev. D **103**, 075028 (2021).

[18] D. Buttazzo and P. Paradisi, Probing the muon g-2 anomaly at a muon collider, arXiv:2012.02769.

[19] W. Yin and M. Yamaguchi, Muon $g-2$ at multi-TeV muon collider, arXiv:2012.03928.

[20] G.-y. Huang, F. S. Queiroz, and W. Rodejohann, Gauged $L_\mu - L_\tau$ at a muon collider, Phys. Rev. D **103**, 095005 (2021).

[21] R. Capdevilla, D. Curtin, Y. Kahn, and G. Krnjaic, A no-lose theorem for discovering the new physics of $(g-2)_\mu$ at muon colliders, arXiv:2101.10334.

[22] G. Bennett *et al.* (Muon g-2 Collaboration), Final report of the muon E821 anomalous magnetic moment measurement at BNL, Phys. Rev. D **73**, 072003 (2006).

[23] B. Roberts, Status of the fermilab muon $(g-2)$ experiment, Chin. Phys. C **34**, 741 (2010).

[24] T. Aoyama *et al.*, The anomalous magnetic moment of the muon in the standard model, Phys. Rep. **887**, 1 (2020).

[25] C. Bobeth, G. Hiller, and G. Piranishvili, Angular distributions of $\bar{B} \to \bar{K}\ell^+\ell^-$ decays, J. High Energy Phys. 12 (2007) 040.

[26] M. Bordone, G. Isidori, and A. Pattori, On the standard model predictions for $R_K$ and $R_{K^*}$, Eur. Phys. J. C **76**, 440 (2016).

[27] B. Capdevila, A. Crivellin, S. Descotes-Genon, J. Matias, and J. Virto, Patterns of new physics in $b \to s\ell^+\ell^-$ transitions in the light of recent data, J. High Energy Phys. 01 (2018) 093.

[28] A. K. Alok, B. Bhattacharya, A. Datta, D. Kumar, J. Kumar, and D. London, New physics in $b \to s\mu^+\mu^-$ after the measurement of $R_{K^*}$, Phys. Rev. D **96**, 095009 (2017).

[29] A. Abdesselam *et al.* (Belle Collaboration), Test of lepton flavor universality in $B \to K\ell^+\ell^-$ decays, J. High Energy Phys. 03 (2021) 105.

[30] A. Abdesselam *et al.* (Belle Collaboration), Test of Lepton Flavor Universality in $B \to K^*\ell^+\ell^-$ Decays at Belle, Phys. Rev. Lett. **126**, 161801 (2021).

[31] J. Aebischer, W. Altmannshofer, D. Guadagnoli, M. Reboud, P. Stangl, and D. M. Straub, $B$-decay discrepancies after Moriond 2019, Eur. Phys. J. C **80**, 252 (2020).

[32] W. Altmannshofer and P. Stangl, New physics in rare B decays after Moriond 2021, Eur. Phys. J. C **81**, 952 (2021).

[33] R. Gauld, F. Goertz, and U. Haisch, An explicit $Z'$-boson explanation of the $B \to K^*\mu^+\mu^-$ anomaly, J. High Energy Phys. 01 (2014) 069.

[34] A. J. Buras, F. De Fazio, and J. Girrbach, 331 models facing new $b \to s\mu^+\mu^-$ data, J. High Energy Phys. 02 (2014) 112.

[35] W. Altmannshofer, S. Gori, M. Pospelov, and I. Yavin, Quark flavor transitions in $L_\mu - L_\tau$ models, Phys. Rev. D **89**, 095033 (2014).

[36] A. Crivellin, G. D'Ambrosio, and J. Heeck, Explaining $h \to \mu^\pm\tau^\mp$, $B \to K^*\mu^+\mu^-$ and $B \to K\mu^+\mu^-/B \to Ke^+e^-$ in a Two-Higgs-Doublet Model with Gauged $L_\mu - L_\tau$, Phys. Rev. Lett. **114**, 151801 (2015).

[37] A. Crivellin, G. D'Ambrosio, and J. Heeck, Addressing the LHC flavor anomalies with horizontal gauge symmetries, Phys. Rev. D **91**, 075006 (2015).

[38] C. Niehoff, P. Stangl, and D. M. Straub, Violation of lepton flavour universality in composite Higgs models, Phys. Lett. B **747**, 182 (2015).

[39] A. Celis, J. Fuentes-Martin, M. Jung, and H. Serodio, Family nonuniversal $Z'$ models with protected flavor-changing interactions, Phys. Rev. D **92**, 015007 (2015).

[40] A. Greljo, G. Isidori, and D. Marzocca, On the breaking of lepton flavor universality in B decays, J. High Energy Phys. 07 (2015) 142.

[41] W. Altmannshofer and I. Yavin, Predictions for lepton flavor universality violation in rare B decays in models with gauged $L_\mu - L_\tau$, Phys. Rev. D **92**, 075022 (2015).

[42] A. Falkowski, M. Nardecchia, and R. Ziegler, Lepton flavor non-universality in B-meson decays from a U(2) flavor model, J. High Energy Phys. 11 (2015) 173.

[43] L. Calibbi, A. Crivellin, F. Kirk, C. A. Manzari, and L. Vernazza, $Z'$ models with less-minimal flavour violation, Phys. Rev. D **101**, 095003 (2020).

[44] A. Carmona and F. Goertz, Lepton Flavor and Nonuniversality from Minimal Composite Higgs Setups, Phys. Rev. Lett. **116**, 251801 (2016).

[45] F. Goertz, J. F. Kamenik, A. Katz, and M. Nardecchia, Indirect constraints on the scalar di-photon resonance at the LHC, J. High Energy Phys. 05 (2016) 187.

[46] C.-W. Chiang, X.-G. He, and G. Valencia, $Z'$ model for $b \to s\ell\bar{\ell}$ flavor anomalies, Phys. Rev. D **93**, 074003 (2016).

[47] D. Bečirević, O. Sumensari, and R. Zukanovich Funchal, Lepton flavor violation in exclusive $b \to s$ decays, Eur. Phys. J. C **76**, 134 (2016).

[48] S. M. Boucenna, A. Celis, J. Fuentes-Martin, A. Vicente, and J. Virto, Non-abelian gauge extensions for B-decay anomalies, Phys. Lett. B **760**, 214 (2016).

[49] S. M. Boucenna, A. Celis, J. Fuentes-Martin, A. Vicente, and J. Virto, Phenomenology of an $SU(2) \times SU(2) \times U(1)$ model with lepton-flavour non-universality, J. High Energy Phys. 12 (2016) 059.

[50] E. Megias, G. Panico, O. Pujolas, and M. Quiros, A natural origin for the LHCb anomalies, J. High Energy Phys. 09 (2016) 118.

[51] I. Garcia Garcia, LHCb anomalies from a natural perspective, J. High Energy Phys. 03 (2017) 040.

[52] P. Ko, Y. Omura, Y. Shigekami, and C. Yu, LHCb anomaly and B physics in flavored $Z'$ models with flavored Higgs doublets, Phys. Rev. D **95**, 115040 (2017).

[53] J. Kawamura, S. Raby, and A. Trautner, Complete vector-like fourth family with U(1)': A global analysis, Phys. Rev. D **101**, 035026 (2020).

[54] E. Megias, M. Quiros, and L. Salas, Lepton-flavor universality violation in $R_K$ and $R_{D^{(*)}}$ from warped space, J. High Energy Phys. 07 (2017) 102.

[55] B. C. Allanach, $U(1)_{B_3-L_2}$ explanation of the neutral current $B$-anomalies, Eur. Phys. J. C **81**, 56 (2021).

[56] L. Di Luzio, M. Kirk, A. Lenz, and T. Rauh, $\Delta M_s$ theory precision confronts flavour anomalies, J. High Energy Phys. 12 (2019) 009.

[57] L. Di Luzio, M. Kirk, and A. Lenz, Updated $B_s$-mixing constraints on new physics models for $b \to s\ell^+\ell^-$ anomalies, Phys. Rev. D **97**, 095035 (2018).

[58] G. Aad *et al.* (ATLAS Collaboration), Search for new non-resonant phenomena in high-mass dilepton final states with the ATLAS detector, J. High Energy Phys. 11 (2020) 005.

[59] D. Beghin (CMS Collaboration), Searches for new resonances decaying to leptons, photons or jets with CMS, Proc. Sci., EPS-HEP2019 (**2020**) 569.

[60] J. P. Lees *et al.* (*BABAR* Collaboration), Search for $B \to K^{(*)}\nu\bar{\nu}$ and invisible quarkonium decays, Phys. Rev. D **87**, 112005 (2013).

[61] G. W. Bennett *et al.* (Muon g-2 Collaboration), Measurement of the Negative Muon Anomalous Magnetic Moment to 0.7 ppm, Phys. Rev. Lett. **92**, 161802 (2004).

[62] F. S. Queiroz and W. Shepherd, New physics contributions to the muon anomalous magnetic moment: A numerical code, Phys. Rev. D **89**, 095024 (2014).

[63] W. Altmannshofer, S. Gori, M. Pospelov, and I. Yavin, Neutrino Trident Production: A Powerful Probe of New Physics with Neutrino Beams, Phys. Rev. Lett. **113**, 091801 (2014).

[64] B. Allanach, F. S. Queiroz, A. Strumia, and S. Sun, $Z'$ models for the LHCb and $g-2$ muon anomalies, Phys. Rev. D **93**, 055045 (2016); Erratum, Phys. Rev. D **95**, 119902 (2017).

[65] F. del Aguila, M. Chala, J. Santiago, and Y. Yamamoto, Collider limits on leptophilic interactions, J. High Energy Phys. 03 (2015) 059.

[66] G. Hiller and M. Schmaltz, $R_K$ and future $b \to s\ell\ell$ physics beyond the standard model opportunities, Phys. Rev. D **90**, 054014 (2014).

[67] B. Gripaios, M. Nardecchia, and S. A. Renner, Composite leptoquarks and anomalies in $B$-meson decays, J. High Energy Phys. 05 (2015) 006.

[68] I. de Medeiros Varzielas and G. Hiller, Clues for flavor from rare lepton and quark decays, J. High Energy Phys. 06 (2015) 072.

[69] D. Bečirević, S. Fajfer, and N. Košnik, Lepton flavor nonuniversality in $b \to s\ell^+\ell^-$ processes, Phys. Rev. D **92**, 014016 (2015).

[70] R. Alonso, B. Grinstein, and J. Martin Camalich, Lepton universality violation and lepton flavor conservation in $B$-meson decays, J. High Energy Phys. 10 (2015) 184.

[71] M. Bauer and M. Neubert, Minimal Leptoquark Explanation for the $\mathrm{R}_{D^{(*)}}$, $\mathrm{R}_K$, and $(g-2)_g$ Anomalies, Phys. Rev. Lett. **116**, 141802 (2016).

[72] S. Fajfer and N. Košnik, Vector leptoquark resolution of $R_K$ and $R_{D^{(*)}}$ puzzles, Phys. Lett. B **755**, 270 (2016).

[73] R. Barbieri, G. Isidori, A. Pattori, and F. Senia, Anomalies in $B$-decays and $U(2)$ flavour symmetry, Eur. Phys. J. C **76**, 67 (2016).

[74] D. Bečirević, N. Košnik, O. Sumensari, and R. Zukanovich Funchal, Palatable leptoquark scenarios for lepton flavor violation in exclusive $b \to s\ell_1\ell_2$ modes, J. High Energy Phys. 11 (2016) 035.

[75] D. Bečirević, S. Fajfer, N. Košnik, and O. Sumensari, Leptoquark model to explain the $B$-physics anomalies, $R_K$ and $R_D$, Phys. Rev. D **94**, 115021 (2016).

[76] A. Crivellin, D. Müller, and T. Ota, Simultaneous explanation of $R(\mathrm{D}^{(*)})$ and $\mathrm{b} \to \mathrm{s}\mu^+\mu^-$: The last scalar leptoquarks standing, J. High Energy Phys. 09 (2017) 040.

[77] G. Hiller and I. Nisandzic, $R_K$ and $R_{K^*}$ beyond the standard model, Phys. Rev. D **96**, 035003 (2017).

[78] D. Bečirević and O. Sumensari, A leptoquark model to accommodate $R_K^{\mathrm{exp}} < R_K^{\mathrm{SM}}$ and $R_{K^*}^{\mathrm{exp}} < R_{K^*}^{\mathrm{SM}}$, J. High Energy Phys. 08 (2017) 104.

[79] I. Doršner, S. Fajfer, D. A. Faroughy, and N. Košnik, The role of the $S_3$ GUT leptoquark in flavor universality and collider searches, J. High Energy Phys. 10 (2017) 188.

[80] N. Assad, B. Fornal, and B. Grinstein, Baryon number and lepton universality violation in leptoquark and diquark models, Phys. Lett. B **777**, 324 (2018).

[81] G. D'Amico, M. Nardecchia, P. Panci, F. Sannino, A. Strumia, R. Torre, and A. Urbano, Flavour anomalies after the $R_{K^*}$ measurement, J. High Energy Phys. 09 (2017) 010.

[82] D. Marzocca, Addressing the B-physics anomalies in a fundamental composite Higgs model, J. High Energy Phys. 07 (2018) 121.

[83] M. Blanke and A. Crivellin, $B$ Meson Anomalies in a Pati-Salam Model within the Randall-Sundrum Background, Phys. Rev. Lett. **121**, 011801 (2018).

[84] L. Di Luzio, A. Greljo, and M. Nardecchia, Gauge leptoquark as the origin of B-physics anomalies, Phys. Rev. D **96**, 115011 (2017).

[85] L. Calibbi, A. Crivellin, and T. Li, Model of vector leptoquarks in view of the $B$-physics anomalies, Phys. Rev. D **98**, 115002 (2018).

[86] M. Bordone, C. Cornella, J. Fuentes-Martin, and G. Isidori, A three-site gauge model for flavor hierarchies and flavor anomalies, Phys. Lett. B **779**, 317 (2018).

[87] S. Saad and A. Thapa, Common origin of neutrino masses and $R_{D^{(*)}}$, $R_{K^{(*)}}$ anomalies, Phys. Rev. D **102**, 015014 (2020).

[88] K. S. Babu, P. S. B. Dev, S. Jana, and A. Thapa, Unified framework for $B$-anomalies, muon $g-2$, and neutrino masses, J. High Energy Phys. 03 (2021) 179.

[89] F. S. Queiroz, K. Sinha, and A. Strumia, Leptoquarks, dark matter, and anomalous LHC events, Phys. Rev. D **91**, 035006 (2015).

[90] A. Angelescu, D. Bečirević, D. A. Faroughy, and O. Sumensari, Closing the window on single leptoquark solutions to the $B$-physics anomalies, J. High Energy Phys. 10 (2018) 183.

[91] S. Davidson, D. C. Bailey, and B. A. Campbell, Model independent constraints on leptoquarks from rare processes, Z. Phys. C **61**, 613 (1994).

[92] I. Doršner, S. Fajfer, A. Greljo, J. F. Kamenik, and N. Košnik, Physics of leptoquarks in precision experiments and at particle colliders, Phys. Rep. **641**, 1 (2016).

[93] G. Aad *et al.* (ATLAS Collaboration), Search for pairs of scalar leptoquarks decaying into quarks and electrons or muons in $\sqrt{s} = 13$ TeV $pp$ collisions with the ATLAS detector, J. High Energy Phys. 10 (2020) 112.

[94] B. C. Allanach, T. Corbett, and M. Madigan, Sensitivity of future hadron colliders to leptoquark pair production in the di-muon di-jets channel, Eur. Phys. J. C **80**, 170 (2020).

[95] A. Greljo and D. Marzocca, High-$p_T$ dilepton tails and flavor physics, Eur. Phys. J. C **77**, 548 (2017).

[96] A. Angelescu, D. Bečirević, D. A. Faroughy, F. Jaffredo, and O. Sumensari, On the single leptoquark solutions to

the $B$-physics anomalies, Phys. Rev. D **104**, 055017 (2021).
[97] CMS Collaboration, Search for a narrow resonance in high-mass dilepton final states in proton-proton collisions using 140 fb$^{-1}$ of data at $\sqrt{s} = 13$ TeV, Report No. CMS-PAS-EXO-19-019, 2019.
[98] M. Aaboud *et al.* (ATLAS Collaboration), Measurements of b-jet tagging efficiency with the ATLAS detector using $t\bar{t}$ events at $\sqrt{s} = 13$ TeV, J. High Energy Phys. 08 (2018) 089.
[99] B. Auerbach, S. Chekanov, J. Love, J. Proudfoot, and A. V. Kotwal, Sensitivity to new high-mass states decaying to $t\bar{t}$ at a 100 TeV collider, Phys. Rev. D **91**, 034014 (2015).
[100] C. Helsens, D. Jamin, M. L. Mangano, T. G. Rizzo, and M. Selvaggi, Heavy resonances at energy-frontier hadron colliders, Eur. Phys. J. C **79**, 569 (2019).
[101] B. Lillie, L. Randall, and L.-T. Wang, The bulk RS KK-gluon at the LHC, J. High Energy Phys. 09 (2007) 074.
[102] R. Mertig, M. Bohm, and A. Denner, FeynCalc: Computer algebraic calculation of Feynman amplitudes, Comput. Phys. Commun. **64**, 345 (1991).
[103] V. Shtabovenko, R. Mertig, and F. Orellana, New developments in FeynCalc 9.0, Comput. Phys. Commun. **207**, 432 (2016).
[104] V. Shtabovenko, R. Mertig, and F. Orellana, FeynCalc 9.3: New features and improvements, Comput. Phys. Commun. **256**, 107478 (2020).
[105] T. Hahn, Generating Feynman diagrams and amplitudes with FeynArts 3, Comput. Phys. Commun. **140**, 418 (2001).
[106] ATLAS Collaboration, A new tagger for the charge identification of b-jets, Report No. ATL-PHYS-PUB-2015-040, 2015, https://inspirehep.net/literature/1795358.